https://jssr.ui.ac.ir/?lang=en

Journal of Stratigraphy and Sedimentology Researches
E-ISSN: 2423-8007
Vol. 39, Issue 4, No. 93, Winter 2024, pp 13-26
Received: 28.03.2023 Accepted: 19.09.2023

Research Paper

Study of source geochemical effects on brine hydrogeochemical changes of the Bajestan Playa, northeast Iran

Sedighe Haghighi Gorji
Department of Geology, Mashhad Branch, Islamic Azad University, Mashhad, Iran
gorjimine@yahoo.com
Habib Alah Torshizian
Associate Professor, Department of Geology, Mashhad Branch, Islamic Azad University, Mashhad, Iran
htorshizian@yahoo.com
Mohammad Javanbakht*
Associate Professor, Department of Geology, Mashhad Branch, Islamic Azad University, Mashhad, Iran
javanbakht3592@mshdiau.ac.ir
Vahid Khademi
Ph.D. student in Tectonics, Department of Geology, Birjand University, Iran
v1362@yahoo.com

Abstract
This research aims to investigate the hydrogeochemical changes and brine evolution process in dry areas, using the Bajestan Playa as a case study. The Bajestan playa is one of the largest playas in the Middle East, located in northeastern Iran within the Central Iran Plate. The playa is surrounded by volcanoclastic rocks and has an arcuate shape with a gentle slope from the margins to the center. The climate of the region is arid and the area belongs to the "D" type in Geomorphological classification. We collected and analyzed 35 samples by the XRF method in September 1998. The results showed that group (1) potassium, calcium, sulfate and magnesium ions; Group (2) of chlorine and sodium ions and group (3) of carbonate and bicarbonate were formed. The spatial distribution of elements indicated that group (1) elements were more prevalent in the south and central parts of the area, group (2) elements were more abundant in the north and east parts, and group (3) elements were more dominant in the west part. The current facies of the playa brine is magnesium sulfate, and the possible evolution paths are I, II, IIIA, IIIB, IIIC. Therefore, we can expect sodium chloride facies for the playa brine in the future. We concluded that the origin and evolution of water resources were the main factors affecting the hydrogeochemical changes of the Bajestan Playa brine.
Keywords: Brine, Bajestan Playa, Hydrogeochemistry, Origin, Chemical weathering

Introduction

The origin of the brines in dry regions is a key factor for understanding the geochemical evolution of saline lakes and playas (Krinsely 1970). These brines are influenced by the inflow waters that enter the closed basins, which can have different sources such as rainfall and groundwater discharge (Deocampo and Jones 2014; Unglert et al. 2016; Yuan et al. 2022). The sediments of these lakes and playas are important for the global carbon cycle, as they store a large amount of carbon and increase its pool over time (Tranvi et al. 2009). Moreover, these sediments contain valuable industrial minerals, such as carbonates, chlorides, and sulfates, as well as minor minerals like barite and celestine, which can affect the concentration of other elements in the environment (Deocampo and Jones 2014; Argamasilla et al. 2017; Rosenberg et al. 2018; Qin et al. 2021; Li et al. 2022). In Iran, the research on saline lakes and playas is relatively recent (Pakzad and Ajalloeian 2004; Erfanian et al. 2020). One of the main playas in Iran and the Middle East is the Bajestan Playa, which covers an area of about 3725 km^2 (Torshizian et al. 2009; Kim et al. 2017). The study area is located in a dry climate region. This study aims to investigate the effect of rocks on geochemical and water evolution trends in hydrogeochemical changes of brines in the Bajestan Playa.

Geological setting

The study area is located in northeastern Iran in a dry climate region with an arcuate shape at 57° 20′ to 58° 30′ Eastern longitude and 34° to 35° Northern latitude (Figure 1). In

*Corresponding author
Haghighi Gorji S. Torshizian H. A. Javanbakht M. & Khdemi V. (2024). Study of source geochemical effects on brine hydrogeochemical changes of the Bajestan Playa, northeast Iran. Journal of Stratigraphy and Sedimentology Researches, 39(4):13-26. doi: 10.22108/jssr.2023.137202.1257

https://doi.org/10.22108/jssr.2023.137202.1257

general, the total slope of the playa decreases from the heights around the playa to its center. This playa is a part of the subcontinent of Central Iran, which is located in the south of the Great Desert Fault, between Dorouneh village in the west and Kashmar city in the east. Despite the small area of the outcrops and the wide area of the desert, all the sub-zones related to the central Iranian subcontinent zone appear together with the fault lines in the extent of the sheet. The southeastern part of the salt desert area is discontinuously and progressively covered by conglomerate, marl, clayey limestones and Cretaceous strata and fossiliferous limestones, which are related to the Lut Block. In this area, the sedimentary rock units are covered by medium to acidic lavas and pyroclastic facies of the Eocene age.

Among the characteristics of this region, relatively high dryness of the air, lack of humidity, rainfall, high evaporation and lack of vegetation can be mentioned. The difference in altitude in the area, from more than 2000 meters to less than 800 meters in the north, west and northeast, caused the difference in weather. The absolute maximum temperature is 28.5 and the minimum temperature is 4 Celsius degrees.

The Bajestan playa with an approximate area of 3725 km^2 is the second largest playa of Iran and one of the main playas in the Middle East (Torshizian et al. 2009). This playa is part of the Lut Block (Krinsely 1970), which is located in the south of the Great Desert Fault. In the area, a series of volcanoclastic rocks including pyroclastic and to a lesser extent epiclastic rocks have outcropped.

With the exception of the Precambrian granitic Doran assemblage (pCgr) which is exposed in the northwest of this area, the oldest known rock unit in the region is the sandstones of the Lalun Formation (Cl). Another Paleozoic formation in the Bajestan Playa is the Jamal Formation (Pj). Mesozoic stratigraphic units including (Ktzl), (Kl), and (Jq) units are mostly carbonates. The Tertiary rocks are the result of magmatic activities that are exposed as volcanic and plutonic igneous rocks in the region. The Quaternary sediments include river alluvium, clay-salt zones, and sand dunes (Figure 2).

The surface and possibly underground currents are connected with the rock units around the playa, during which elements and particles are separated from the source and deposited in the playa. Along with the movement of underground water into the ground, elements may be added to the soils of the region or dissolved from these soils, leading to a change in their chemical composition.

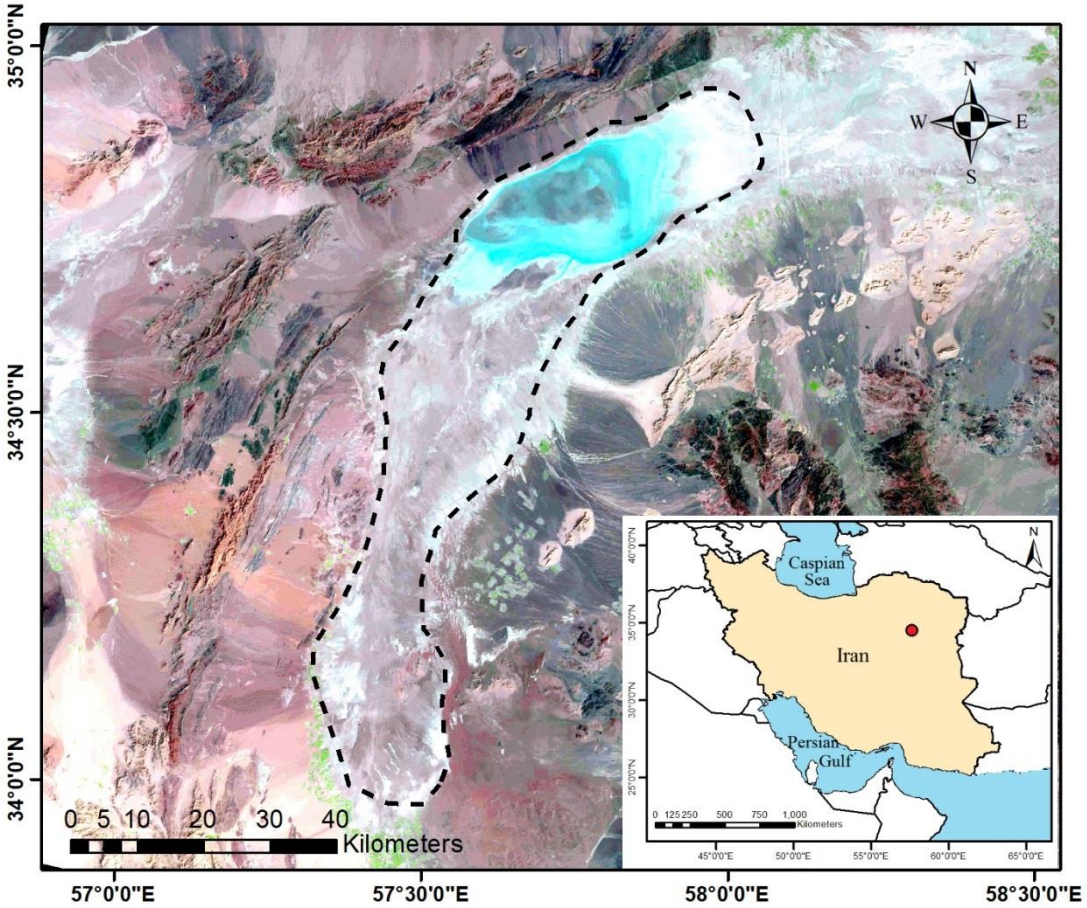

Fig 1- Geographical map of Iran with the location of the study area (A) and satellite image of the Bajestan Playa and surrounding area (B).

https://doi.org/10.22108/jssr.2023.137202.1257

Method

We conducted field studies in the Bajestan Playa for a week in September 2019. We used a hand rotary machine to drill and collect 35 brine samples from a depth of one meter (Figure 2). We analyzed the evaporate samples in the laboratory by XRF method (XRF-1800 Series in Lab Center of Iran Mineral Processing Research Center). We also measured the physicochemical properties of the brines, such as pH, T.H and T.D.S, by standard method 2540 (Table 1) in the IMIDRO company's laboratories in Karaj,Iran.(The total hardness was measured by titration method, total dissolved solids (TDS) by heating method and pH was measured by pH meter. We used various software, such as Excell, Geochemistry Good, GIS10.3 and Rockwork v. 16, to analyze the data and draw diagrams, tables as well as the element isoconcentration maps. We used Piper (1944) diagrams to classify the samples and determine the water chemical type. The total amount and percentage of anions and cations are shown on the side triangles and their corresponding points are plotted on the middle rhombus. The Piper diagram indicates the water quality type based on the concentration area.

The chemical composition and concentration of the water samples were compared using Stiff diagrams, which are graphical representations of the soluble ions. To group the elements based on their similarity or differences, a clustered bar chart was created in SPSS software. This chart shows the correlation between the elements and separates the samples into sub-clusters with lines. The elements within each sub-cluster have the highest similarity. Clustered bar charts were made for all the anions and cations of the brine samples (Miller and Miller 2000).

The covariance matrix was used to obtain the principal components, which are linear combinations of the original variables that account for most of the variance in the data. Principal component analysis is a technique that reduces the dimensionality of the data by transforming it into a few uncorrelated components (Boruvka et al. 2005; Kai et al. 2021). Simeonov et al. (2000) applied this technique to extract more information on the relationships between sampling sites, pollutant concentrations, latent factors and pollutant sources.

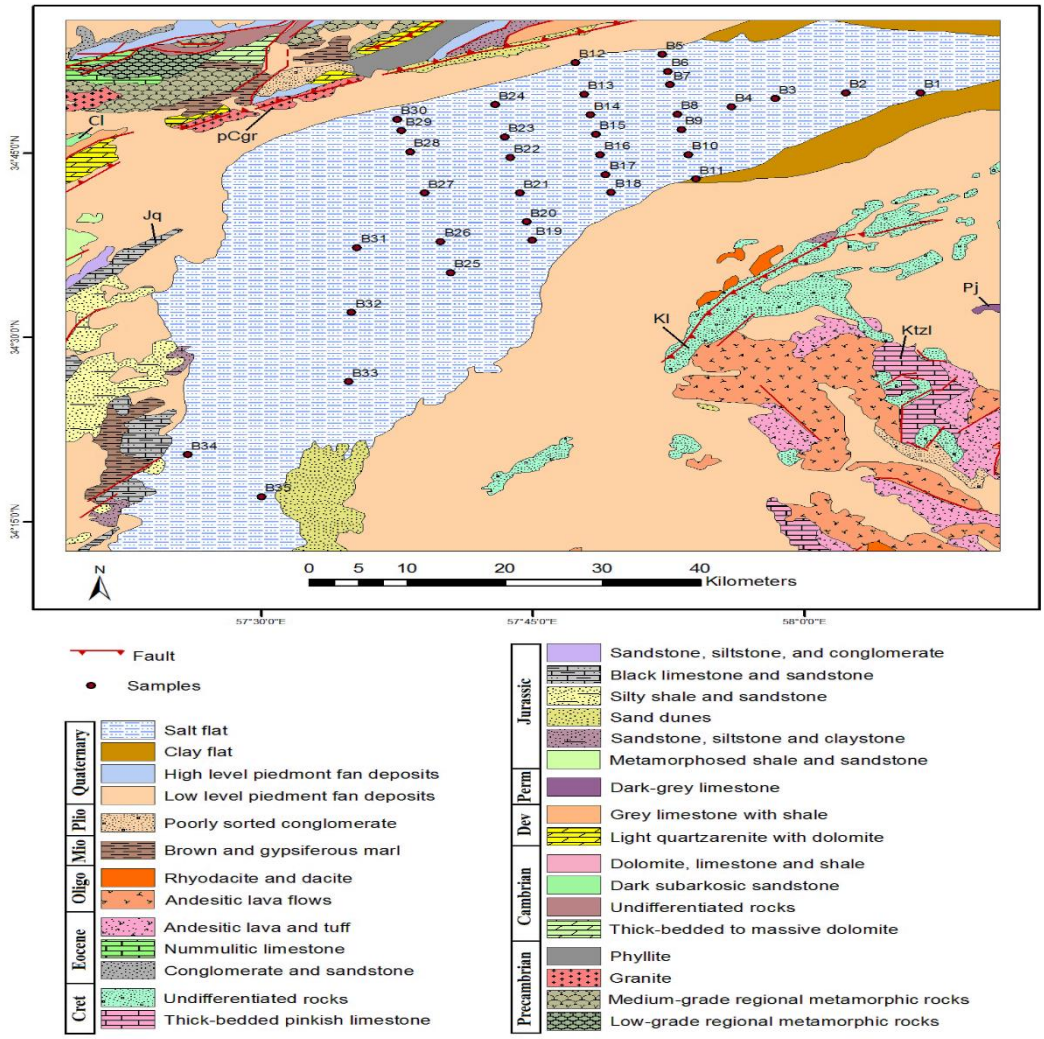

Fig 2- Geological map of the study area with plotted sampling locations, reproduced from Eftekhar-Nezhad and Ruttner (1977).

https://doi.org/10.22108/jssr.2023.137202.1257

Table 1- Physicochemical analysis of samples collected from the Bajestan Playa, NE Iran.

Sample No	X(UTM)	Y(UTM)	PH	T.D.S (mg/l)	T.H (mg/l CaCo3)	$HCO3^{-}$ (ppm)	$CO3^{2-}$ (ppm)	Cl^{-} (ppm)	$SO4^{2-}$ (ppm)	Na^{+} (ppm)	K^{+} (ppm)	Mg2+ (ppm)	Ca2+ (ppm)
B1	6442082	607953.6	7.2	142.1	14.61	7	0	90.2	4796	38	185	1530	1310
B2	6434383	608162.6	7.3	168	11.34	6	0	110	4677	50	300	791/3	1275
B3	607882.5	607882.5	6.8	305.5	19.4	5	0	184	2527	93.33	420	2163	1655
B4	6422665	607344.8	6.8	310.8	22.24	4	0	188	2970	93.33	520	2743	1723
B5	6415669	611753.2	7.3	217.7	18.53	3	0	135	3780	56	440	2163	1517
B6	6416188	610370.4	7	340.1	30.96	2	0	180	2650	76	925	5012	1620
B7	6416375	609293.8	7	322.6	44.25	2	0	206	1840	80	950	7122	2344
B8	6417084	606901.1	6.9	346.3	45.78	1	0	206	2430	84	775	6225	3171
B9	6417515	605653.7	6.4	355	21.15	1	0	210	3580	92	780	2585	1655
B10	6418112	603611.4	7.3	345.4	27.03	1	0	214	3640	92	1100	3218	2172
B11	6418866	601648.2	7.3	380.5	33.27	2	0	212	3680	88	1550	4991	1999
B12	6406747	611340.6	6.9	342.9	31.61	5	0	210	4630	88	1600	5539	1379
B13	6407574	608773.5	6.6	434.5	129.7	6	0	218	1350	62	3100	19203	4826
B14	6408178	607088.9	7.1	369.1	20.49	4	0	222	3646	95	850	2954	1310
B15	6408694	605522.7	7	362.1	25.94	2	0	196	2712	84	1050	4537	1137
B16	6409114	603843.9	7	382	25.51	0	0	204	3222	88	1100	4590	1034
B17	6409630	602229	7	383.7	79.79	0	0	204	1531	68	2700	14930	2661
B18	6410151	600796.1	7.1	336.2	27.03	0	0	192	2366	88	850	2216	2826
B19	6401924	597131.7	6.7	391.9	63.44	1	0	19.2	1745	76	2000	11923	2240
B20	6401403	598633.1	6.7	399.1	83.93	2	0	204	1564	70	3000	15827	2930
B21	6400780	600964.8	7.2	342	31.61	4	0	200	2778	88	1100	5645	1310
B22	6399864	603850.9	7.1	334.5	26.6	5	0	216	2757	10	580	3798	1723
B23	6399351	605536	7.1	338.3	24.2	3	0	192	3140	88	950	2269	2344
B24	6398430	608176.2	7.1	336.2	19.62	2	0	192	3082	88	800	2648	1372
B25	6393513	594698.8	7	353.5	42.29	0	0	208	2872	92	1900	4854	3516
B26	6392583	597240.6	7	338.4	309.6	1	0	196	2699	96	1250	4748	1792
B27	6391010	601209.2	7.4	352.5	18.09	3	0	192	17950	100	680	3324	689
B28	6389642	604595.1	7.4	252.9	12.86	6	0	149	4205	78	135	1899	793
B29	6388790	606343.2	7.3	436.5	100.9	8	0	192	22114	72	1040	22632	1172
B30	6388381	607250.2	6.7	580.7	284.5	10	0	200	37516	33	2200	58032	1379
B31	6383976	596965.6	7.8	146	8.07	190	26	110	7469	42	105	263.8	1103
B32	6383298	591714.5	7	337.2	11.88	8	0	190	4270	108	410	1491	917
B33	6382865	586107.7	6.8	338.1	21.12	5	0	193	5110	104	475	2822	1516
B34	6366264	580503.7	6.8	315	10.88	3	0	159	3980	90	350	1291	717
B35	6373773	576941.8	6.7	338.1	21.12	1	0	193	5110	104	475	2822	1516

Results

The following text summarizes the hydrogeochemical data from the brine samples collected in the Bajestan Playa.

- Physicochemical properties:

The pH of the brine samples ranges from 6.36 to 7.75, indicating a neutral to alkaline condition. The center and west of the playa have the highest pH values, while the east and southeast have the lowest ones (Figure 3A). The total dissolved solids (T.D.S) vary from 0.8 to 31.2 g/L, with the highest value in sample B30 in the northwest and the lowest value in sample B1 in the east of the playa (Figure 3B). The total water hardness also differs from 8.6 to 306.6 mg/L as CaCO3, with sample B26 in the northwest having the highest hardness and sample B31 in the east having the lowest hardness (Figure 3C).

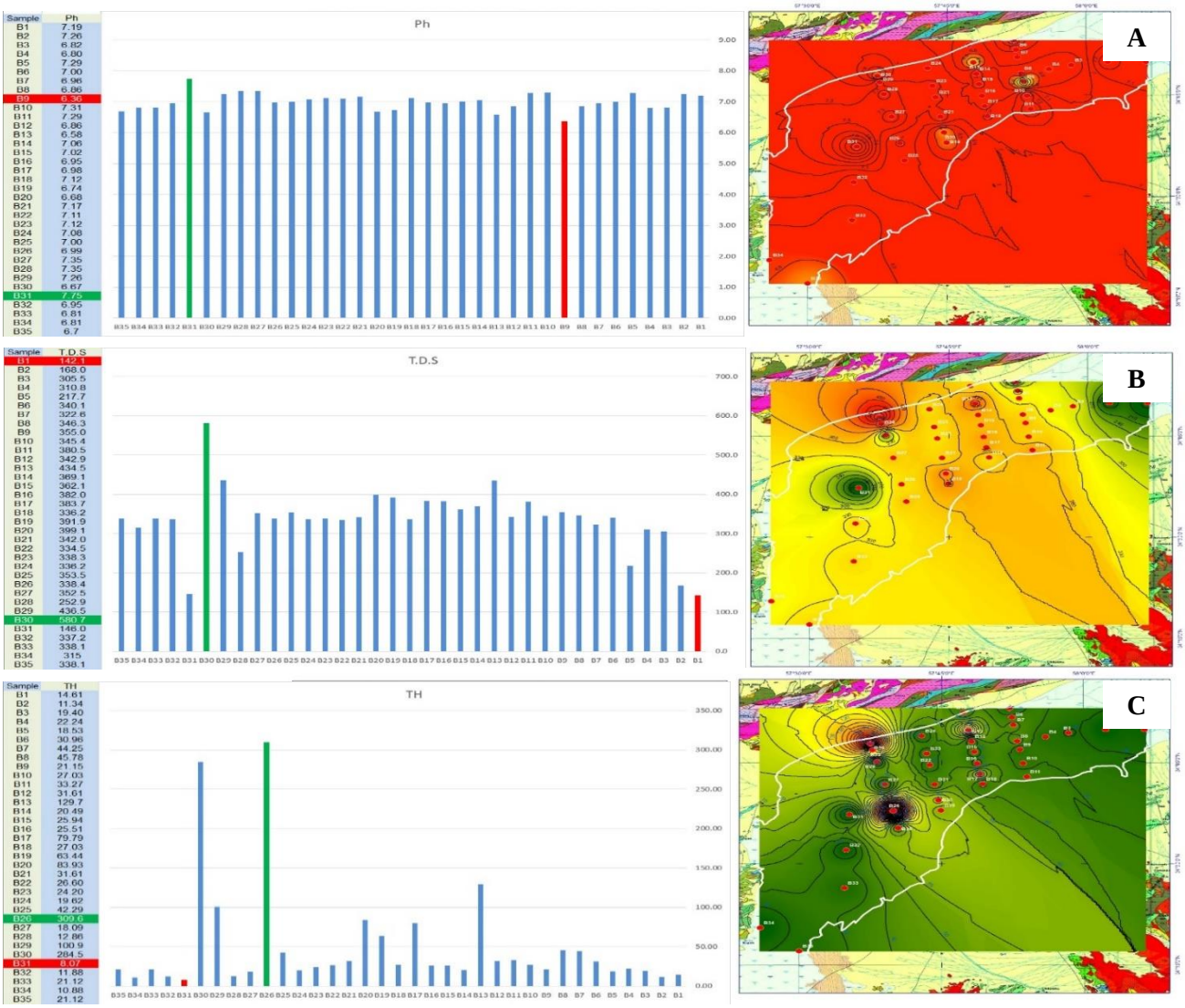

Fig 3- Diagram and zoning map of acidity (pH) (A), total dissolved solids (T.D.S) (B) and total hardness (TH) (C) in the brine samples of the Bajestan Playa, northeast Iran

Anions

Using samples collected from the Bajestan Playa, we analyzed the concentrations of bicarbonate, carbonate, chlorine, and sulfate ions. The results showed that bicarbonate levels varied across the samples, with an average of 8.66 mg/l. The highest bicarbonate concentration was in sample B31, while samples B16, B18, and B25 had the lowest (Figure 4A). Sample B31 also had the highest carbonate concentration, located in the west of the playa (Figure 4B). The chlorine ion concentration ranged from a minimum in sample B19 to a maximum in sample B13 (Figure 4C). The sulfate ion concentration was highest in sample B30, which was in the north of the playa, and lowest in sample B13, which was in the south of the playa (Figure 4D).

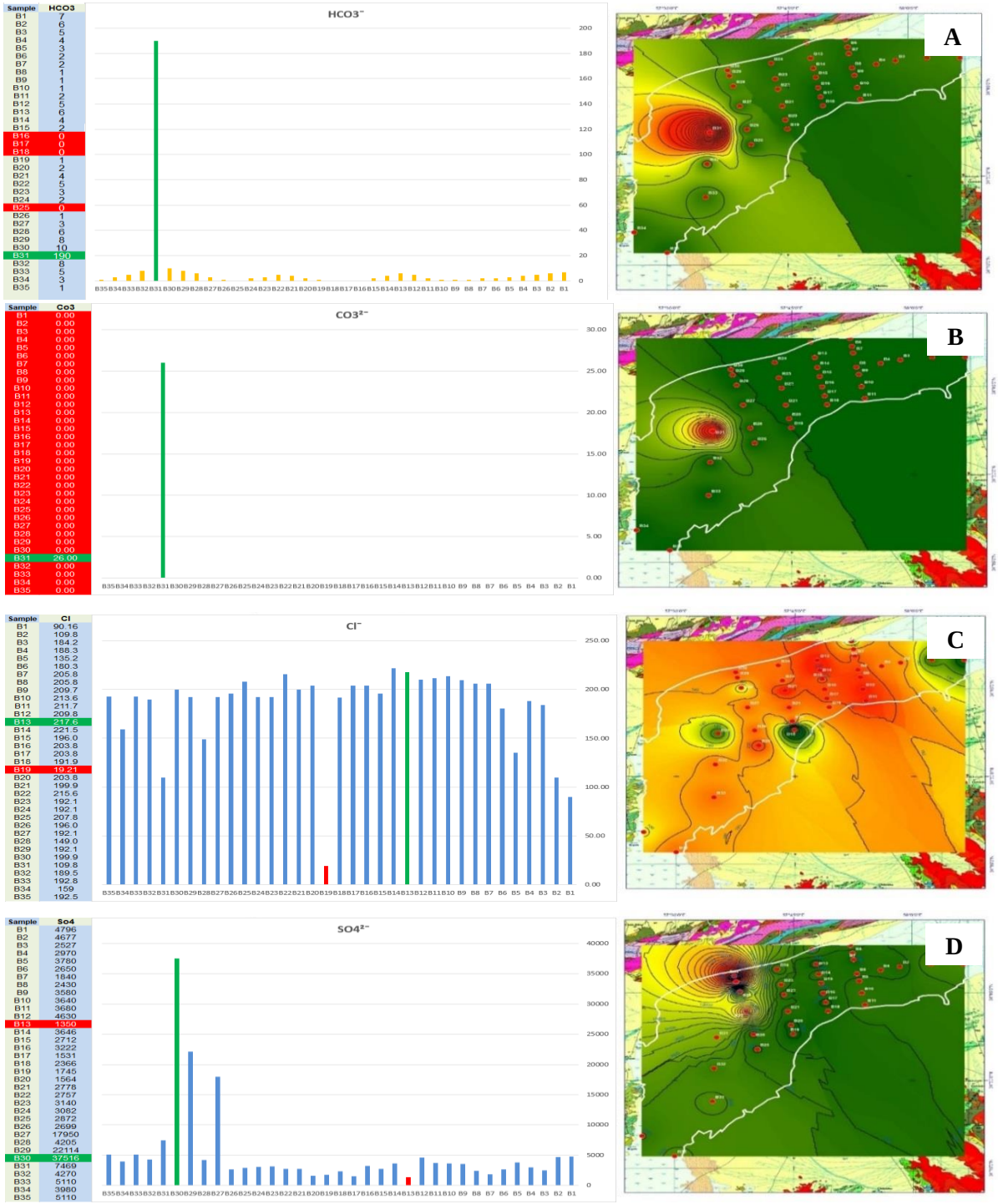

Fig 4- Diagram and zoning map of bicarbonate (A), carbonate (B), chlorine (C) and sulfate (D) in the samples of the Bajestan Playa, northeast Iran.

Cations

The study area was sampled for Na^+, K^+, Mg^{2+} and Ca^{2+} ions. The results showed that sample B32 had the highest Na+ concentration, while sample B22 had the lowest. The spatial distribution of Na^+ was higher in the central, eastern and southern parts of the area, as shown in Figure 5A. For K^+, the highest concentration was found in sample B13, and the lowest in sample B31. The K^+ zoning map (Figure 5B) indicated that the ion was more abundant in the central, northern and southeastern parts of the area. Sample B30 had the highest Mg^{2+} concentration, and sample B31 had the lowest. The Mg^{2+} zoning map (Figure 5C) showed no clear

pattern of spatial variation. For Ca^{2+}, sample B13 had the highest concentration, and sample B27 had the lowest. The Ca^{2+} zoning map (Figure 5D) showed that the ion was more abundant in the northern and western parts of the area.

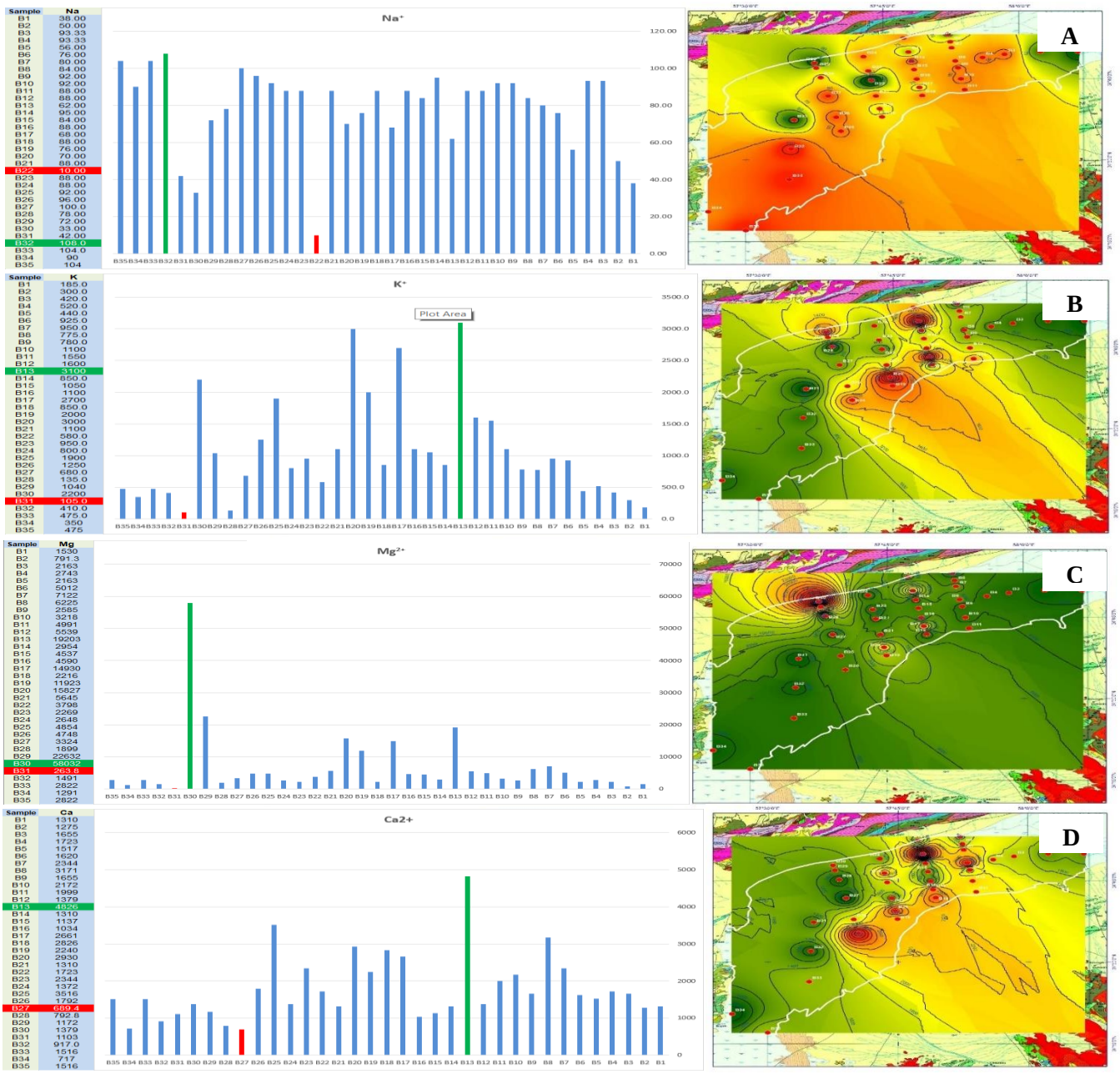

Fig 5- Diagram and zoning map of sodium (A), potassium (B), magnesium (C), and calcium (D) in the samples of the Bajestan Playa, northeast Iran.

Piper diagram

The Piper diagram is a useful tool for comparing the cations and anions in different water samples (Montoya 2018). It can reveal the dominant water facies and the type of salinity. In this study, we analyzed the cations and anions of 34 water samples from different locations (Figure 2). We found that most of the samples belonged to the sulfate facies and had a high concentration of sulfate ions. Only four samples (B2, B18, B23, and B31) deviated from this pattern and showed calcium sulfate facies, as shown in Figure 6. This indicates that these samples had a different origin or underwent a different geochemical process than the rest of the samples.

https://doi.org/10.22108/jssr.2023.137202.1257

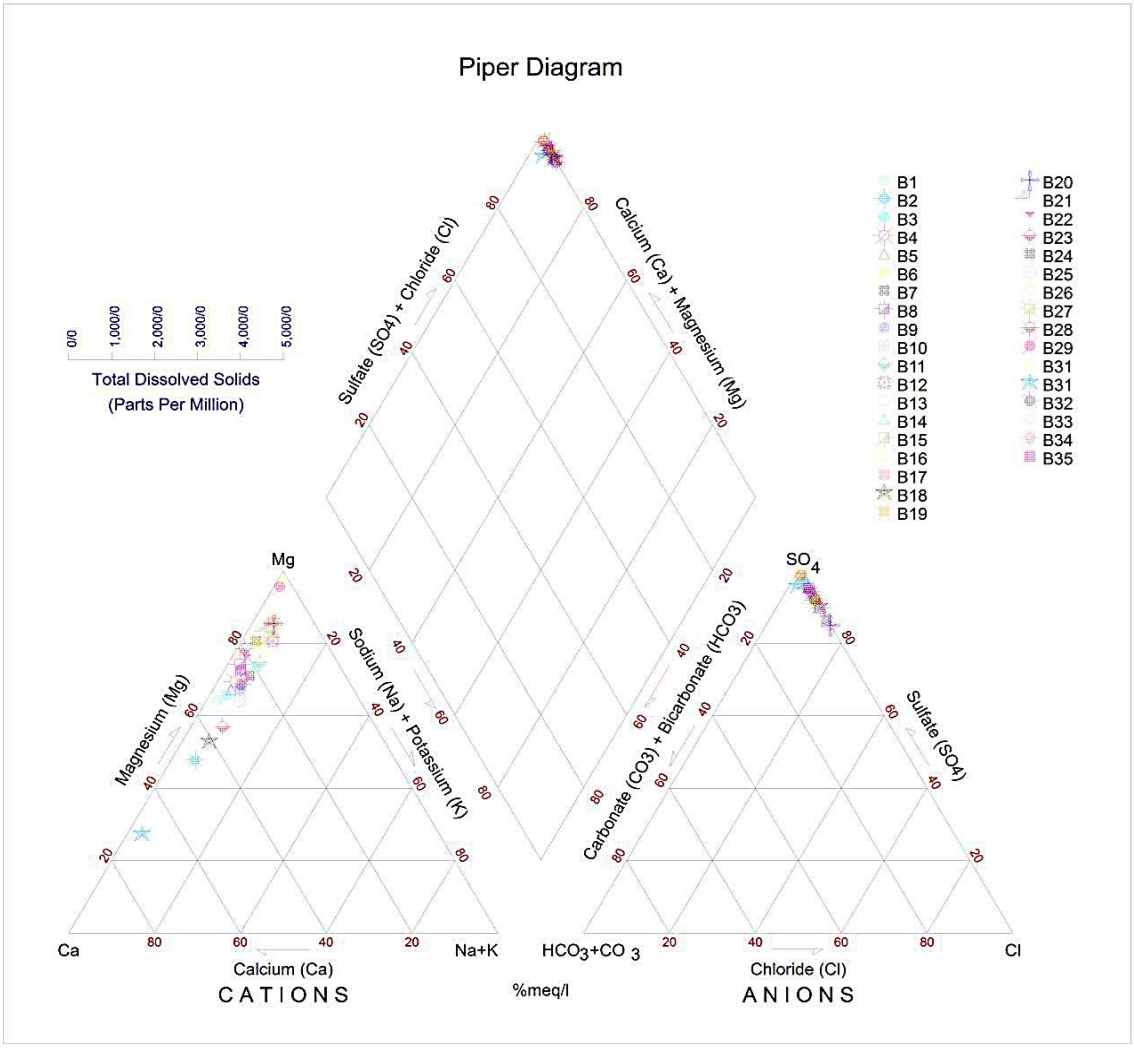

Fig 6- Piper diagrams of samples taken from the Bajestan Playa, northeast Iran (Piper 1944).

Stiff diagram

A Stiff diagram is a graphical tool for comparing the hydrochemical facies and the total soluble solids concentrations of different water samples (Stiff 1951). The diagram plots the anions and cations in milliequivalents per liter on the right and left sides of a vertical axis, respectively. The distance between the ions on the diagram indicates the degree of compatibility or precipitation of cations and anions.

One observation from the diagram is that the magnesium and sulfate ions are farther apart than the other ions, suggesting a higher tendency of magnesium sulfate to form brine (Figure 7).

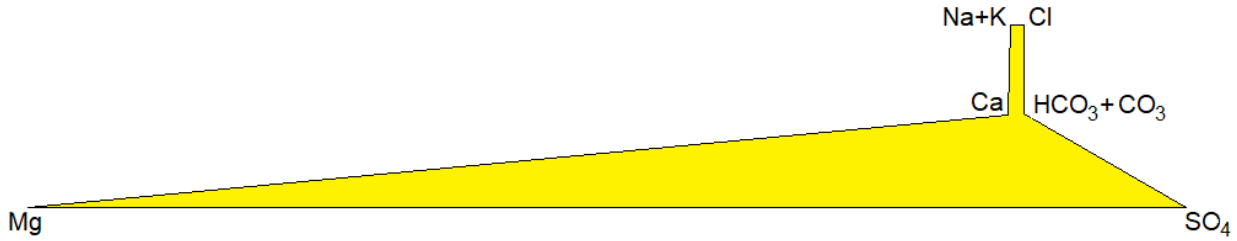

Fig 7- Stiff diagram of the average ions of the brine samples of the Bajestan Playa, northeast Iran. Note the sample shows the type and facies of magnesium sulfate.

Pearson's Correlation Coefficient

The Pearson correlation coefficient matrix for anions and cations in the brine samples is presented in this research (Table 2). The results reveal that most of the elements have a high and positive correlation with each other, suggesting that they share a common source or that they have been enriched by the brine evolution process.

https://doi.org/10.22108/jssr.2023.137202.1257

Table 2- Matrix of correlation values (r) of anions and cations in the samples of the Bajestan Playa, northeast Iran.

Kendall's tau-b	Ca							
Ca	1.000	Mg						
Mg	0.322	1.000	Na					
Na	-0.090	-0.207	1.000	K				
K	0.386	0.690	-0.112	1.000	Cl			
Cl	0.284	0.415	0.113	0.461	1.000	SO_4		
SO_4	-0.170	-0.239	-0.202	-0.240	-0.206	1.000	CO_3	
CO_3	-0.506	-0.345	0.119	-0.340	-0.155	0.197	1.000	HCO_3
HCO_3	-0.378	-0.191	-0.197	-0.330	-0.205	0.411	0.251	1.000

Cluster Analysis Chart (CA)

A cluster diagram of anions and cations in the Bajestan Playa reveals three main clusters, based on their chemical composition and distribution. The first cluster comprises K^+, Ca^{2+}, SO_4^{2-}, and Mg^{2+}, which are further divided into three subclusters according to their relative abundance. The second cluster consists of Cl^- and Na^+, which have a similar spatial pattern. The third cluster includes HCO^{3-} and CO_3^{2-}, which form a distinct subclass (Figure 8).

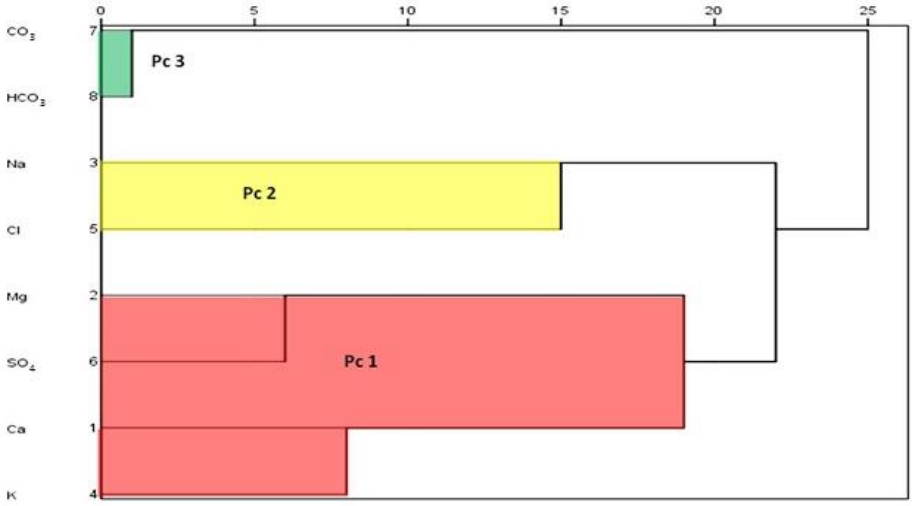

Fig 8- Cluster diagram of the anions and cations in the brine samples of the Bajestan Playa, northeast Iran.

Using principal component analysis (PCA) to determine element dependency

The diagram of principal component analysis for anions and cations of the Bajestan Playa (Figure 9) shows three components: Pc1, Pc2, and Pc3. Pc1 consists of K, Mg, Ca, SO_4, Pc2 comprises Na, Cl, and Pc3 includes HCO_3 and CO_3. There is a weak correlation between Pc1 and Pc2 elements. These components indicate two distinct factors that affect the element accumulation in the brine sources of the study area.

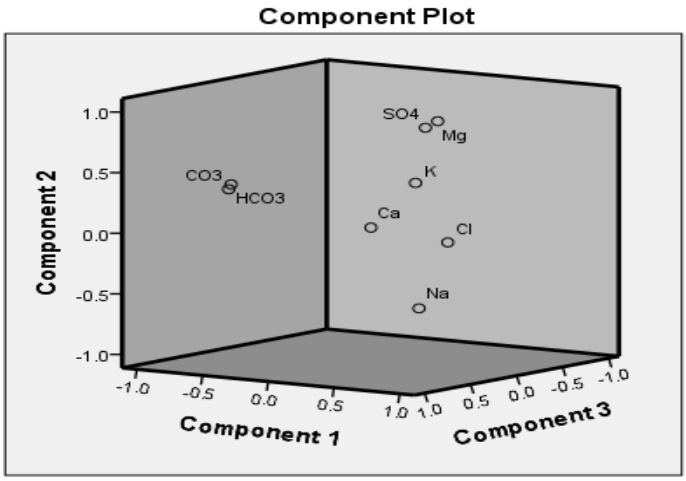

Fig 9- Three-dimensional diagram of principal component analysis for anions and cations in the brine samples of the Bajestan Playa, northeast Iran.

https://doi.org/10.22108/jssr.2023.137202.1257

Discussion

The salinity and composition of lake water depend on the interaction of several factors, such as the type of rocks around the basin, the chemical weathering of these rocks, and the balance of major ions in the water (Deocampo and Jones 2014, Satheeskumar et al. 2021). Different geological formations produce different solutes when they react with natural water (Figure 10). This affects the initial ratio of HCO_3 / Ca+Mg in the water. Based on the flowchart the water may start with high CO_3 and low Ca+Mg, but as sulfides dissolve, the CO_3 decreases and the Ca+Mg increases, which influences the solute evolution of the water (Deocampo and Jones 2014, Argamasilla et al. 2017) (Figure 10).

The study area consists of various rock types from seven groups: evaporates, pyroclastics, carbonates, mafic silicates, plagioclase feldspars, calcite-sulfides and silicate-sulfides (Figure 11). These groups cover different proportions of the total area of the drainage basins in the Bajestan Playa. Group 1 (evaporates) covers 10.5%, group 2 (pyroclastics) covers 0.8%, group 3 (carbonates) covers 4.6%, group 4 (mafic silicates) covers 7.7%, group 5 (plagioclase feldspar) covers 31.3%, group 6 (calcite and sulfides) covers 3%, and group 7 (silicate and sulfides) covers 52.8% of the area.

The chemical analysis of the waters that flow into the Bajestan Playa aquifer reveals that their ionic composition is influenced by the evaporitic formations around the playa and their occurrence frequency. These waters can be classified into three groups according to their dominant anions (Figure 11). Group 1: These waters have high concentrations of $Cl+SO_4$ due to the presence of marl, salt-gypsum and marl limestone formations.

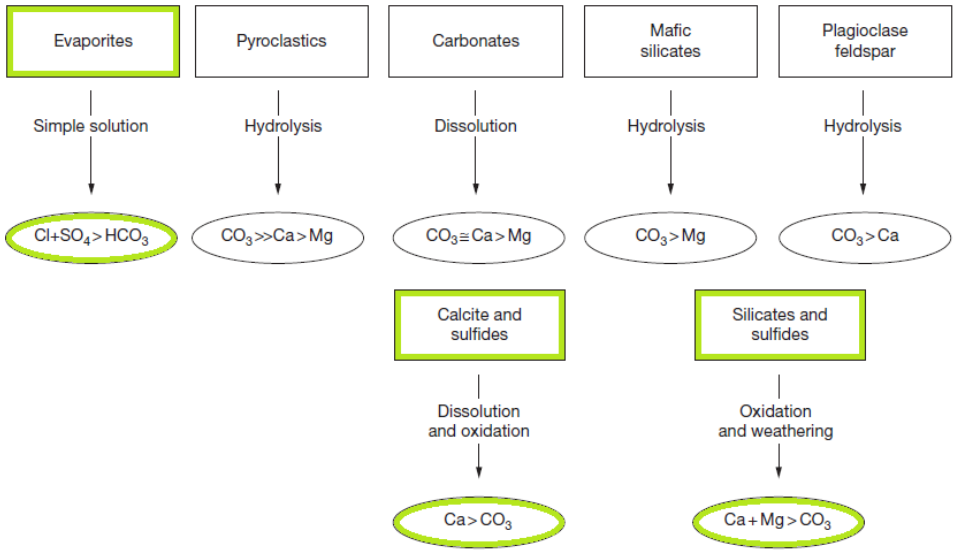

Fig 10- Schematic representation of major fluid types produced by weathering of different rock types, reproduced from Deocampo and Jones (2014)

The quality of water in the Bajestan Playa depends on the hydrogeochemical characteristics of the formations that feed it. The playa receives water from two main branches, which have different geological features. The branches are divided into three zones based on their dominant formations: zone A, B, and C. Zone A covers the north, northwest, and west of the study area and consists of carbonate and shalely formations that contain sulfur, pyrite, and chalcopyrite. These formations increase the carbonate concentration in the water (CO_3> Ca). Zone B covers the east, southeast, and south of the study area and consists of silicate and sulfide formations such as sandstone, shale, and conglomerate. These formations increase the calcium and magnesium concentration in the water (Ca+Mg>CO_3). Zone C covers the northeast of the study area and has a smaller area than the other two zones. The playa is located between zones A and B, which influence its water quality. The water quality changes as it interacts with the upstream formations and leaches their ions.

The lithology of the rocks and sediments that undergo weathering and the long residence time of groundwater within the playa rocks (Eugster and Hardie 1978; Eugster 1980; Deocampo and Jones 2014; Erfanian et al. 2020) influence the sources of ions in the Bajestan playa brine samples. The ions originate from runoff and groundwater that eventually deposit as salt in the basin and elevate the EC of the water in the region. Different cations and anions result from the chemical weathering of various rocks with natural water. According to the analyses by researchers (White and Drake 1993; Cohen 2003 Hao et al. 2020), some examples are:

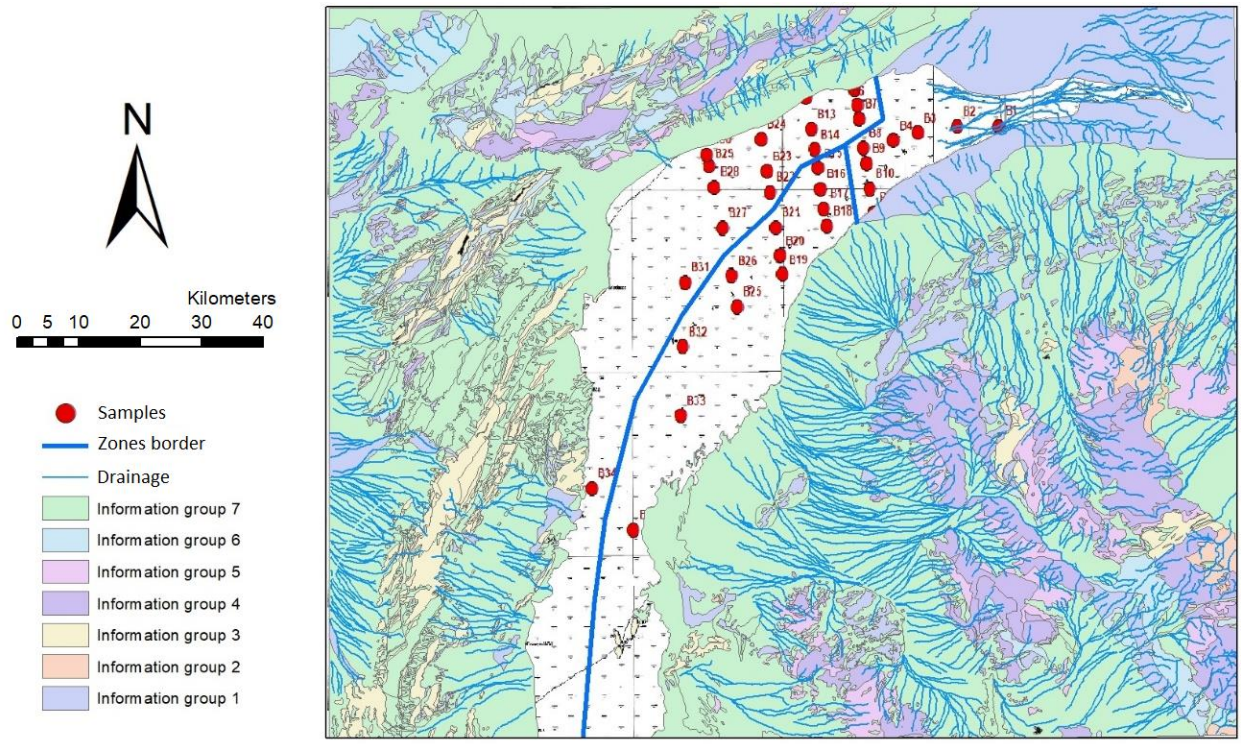

Fig 11- Division of water inflow zones into the study area.

The geochemical content of water is influenced by rock-water interaction. Limestone-rich rocks increase the Ca and pH levels of water while lowering its SiO_2 concentration. The average Ca/Na molar ratio in zone 1, where limestone is more prevalent, is 33.92, compared to 23.11 and 24.78 in zones 2 and 3, respectively. Dolomite-rich rocks have a similar effect, but also add Mg to the water in equal amounts as Ca. The average Mg/Ca molar ratio in zone 3, where dolomite is more dominant, is 0.76, followed by 0.65 in zone 1 and 0.44 in zone 2. The dolomitic lithology has a stronger impact on the water chemistry firstly in zone 3, and secondly in zone 1 and then by zone 2.

The hydrogeochemical characteristics of waters in contact with shale and sandstone are different (Xiao et al. 2021). Water in shales has high HCO and sometimes high SO, with Ca and Na as the main cations. The pH can vary from 4 to 9, depending on the sulfate and carbonate content. The T.D.S is also high, especially for sulfate- and chloride-rich waters. The data from the three zones show that the second zone has the highest average cationic and anionic value (2234.72), indicating a greater influence of shale lithology on water chemistry.

Water in sandstones has more variable cations, but HCO_3 is the dominant anion. The silica content is low and the pH is nearly neutral. The hydrogeochemical analysis of the area reveals that the second zone has the highest bicarbonate content, suggesting that sandstone lithology has also affected the geochemical composition of this zone in the past.

One of the factors that influence the chemical evolution of water in closed basins is the type of inflow water (Mollema et al. 2013). Eugster and Hardy (1978) identified three main types of inflow waters and their effects on the final saline water (Figure 12).

Process I involves waters with very high HCO_3/Ca+Mg ratios (HCO_3 >> Ca+Mg). These waters deposit alkaline carbonates and produce alkaline brines that contain high concentrations of SO_3^{2-}, CO_3^{2-}, HCO_3^-, K^+, Na^-, Cl^- ions (Sallem et al. 2022). These brines can form minerals such as trona, natron, nahcolite, halite, mirabilite, or tenardite (Warren 2006; Chen et al. 2021). Based on the analysis of the Bajestan Playa samples, process I can be considered as one of the evolutionary paths, since most of the samples have Mg> SO_4 and Mg> CO_3, ad no carbonate (CO_3 = 0).

Process II involves inlet waters that have low bicarbonate levels (HCO_3 <<Ca+Mg), which means they are either chlorinated or sulfated. This causes bicarbonate to be quickly removed and alkaline soils to accumulate. Some of the Bajestan Playa brine samples (B2, B18, B23, B31) show this process, as they have gypsum and calcium facies (Ca >>Mg).

Process III occurs when inlet waters have no dominant ions of HCO_3 or Ca+ Mg. In this case, the water can either lose alkaline earth elements or gain bicarbonate. Most of the Bajestan Playa inflow waters follow this process, as they match the "rich in Mg+Ca", "Mg>>Ca", and "poor in HCO_3" conditions, except for some samples that do not have magnesite type and facies or do not satisfy the "Mg>>Ca" criterion (such as B2, B18, B23, B31). Additionally, some samples may follow the IIIC pathway, which leads to gypsum and magnesium silicate formation, unless they have magnesite sulfate type and facies or other types and facies that are incompatible with this process. Gypsum formation is more likely in calcite sulfate facies (Ibrahim et al. 2023).

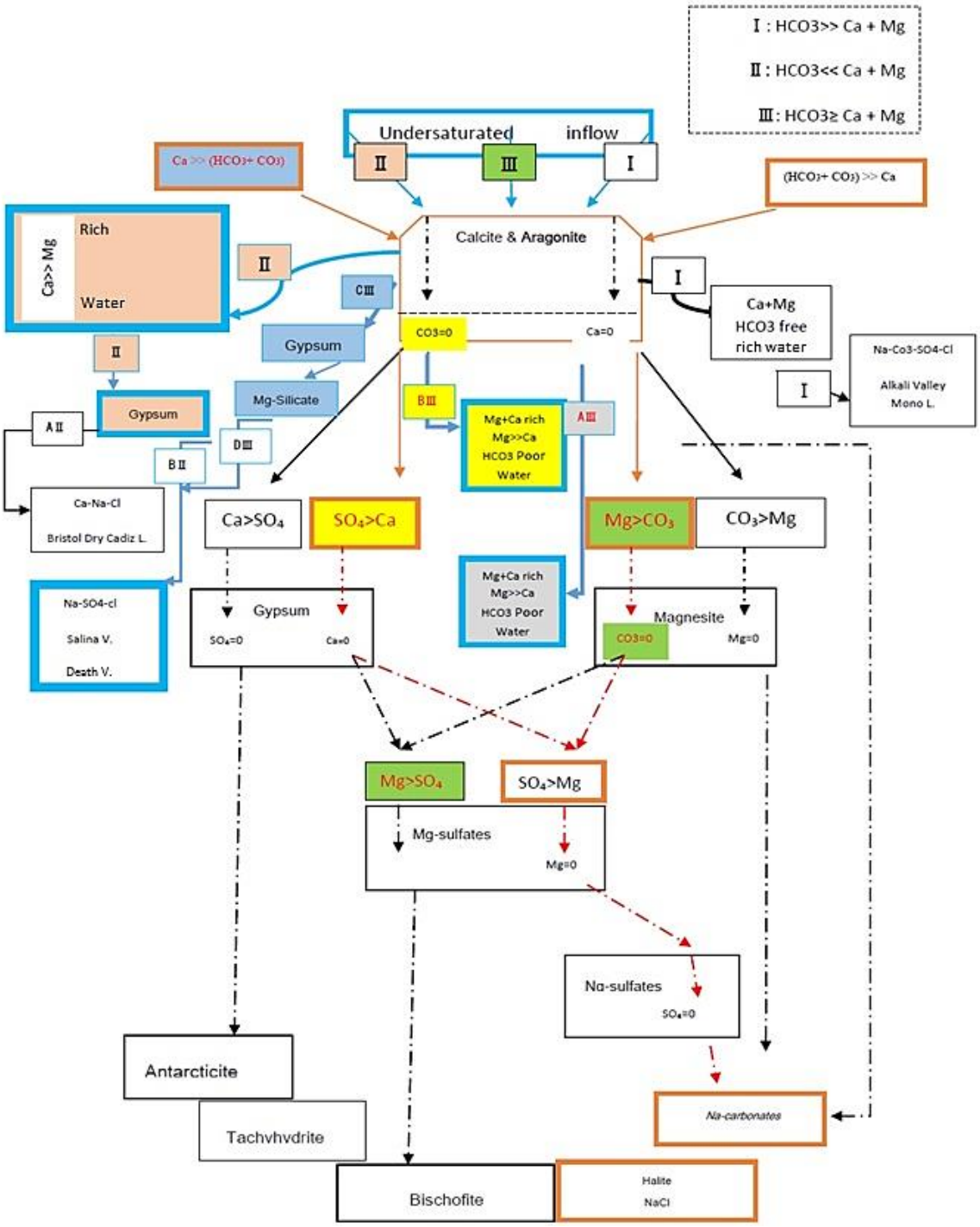

Fig 12- Diagram of brine evolution from non-seawater (Eugster and Hardie 1978; Warren 2006)

Conclusion

The Bajestan Playa due to the presence of large alluvial fans a significant playa in the Middle East region, located in northeastern Iran. To examine how the origin influences the hydrogeochemical variations and evolution of brines, 35 samples were collected and analyzed by the XRF method. The results indicated that the brine samples had relatively neutral pH, lower T.D.S frequency in the center of playa than the surrounding area, and total hardness of water ranging from 8.07 to 306.6. The cation and anion values in this playa revealed that magnesium sulfate was the dominant type and facies. Statistical studies of element dependence identified three main clusters: the first cluster consisted of K, Ca, SO_4, and Mg, with three subgroups; the second cluster comprised Cl, Na; and the third cluster included HCO_3, CO_3, with one subcluster. The Bajestan Playa received water from two main groups, which were divided into three zones based on the feeding formations: Zone A (northern, northwestern,

western), Zone B (eastern, southeastern, southern), and Zone C (northeastern). In general, the waters in Zone 1 had a higher molar Ca/Na ratio than in Zones 2 and 3, suggesting more influence of carbonate formations on their geochemical content. Conversely, the effect of dolomitic lithology was greatest in Zone 3 and least in Zone 2. Mean cationic and anionic values showed that shale lithology had more impact on the hydrogeochemical content of Zone 2. Moreover, Zone 2 had more bicarbonate anion and possibly sandstone lithology had more contribution to its geochemical content at the relevant time. In conclusion, it can be projected that the evolution of the Bajestan Playa brines will follow the trends of I, II, IIIA, IIIB and IIIC in the future. Comparison of the obtained results with similar studies shows that the chemical content of the origin and the evolutionary process of the brines are the two main controlling factors in this playa.

References

Argamasilla M. Barberá J. A. and Andreo B. 2017. Factors controlling groundwater salinization and hydrogeochemical processes in coastal aquifers from southern Spain. Science Total Environment, 580: 50–68.

Boruvka L. Vacek, O. and Jehlicˇka, J. 2005. Principal component analysis as a tool to indicate the origin of potentially toxic elements in soils. Geoderma,128: 289 – 300.

Chen W. Zhang Y. Shi W. Cui Y. Zhang Q. Shi Y. and Liang Z. 2021. Analysis of hydrogeochemical characteristics and origins of chromium contamination in groundwater at a site in Xinxiang City, Henan Province. Applied Science, 11: 11683.

Cohen A. S. 2003. Paleolimnology: The History and Evolution of Lake Systems. Oxford University Press, 500p.

Deocampo D. M. and Jones B. F. 2014. Geochemistry of Saline Lakes. In Treatise on Geochemistry, 437–469.

Eftekha-Nezhad J. and Ruttner A. 1977. 1:250,000 Geological map of Ferdows. Geological Survey of Iran.

Erfanian Kaseb H. Torshizian H. Jahani D. Javanbakht M. and Kohansal Ghadimvand N. 2020. Effects of lithological and evolutionary processes on geochemical changes of Shahrokht-Yazdan Playa brines (east of Iran-west of Afghanistan). Arabian Journal of Geosciences, 13: 1070-1083.

Erfanian kaseb H. Torshizian H. Jahani D. Javanbakht M. and Kohansal Ghadimvand N. 2020. Studying evolutionary processes of Petergan Playa brines in south Khorasan, east of Iran. Geopersia, 10: 333-349.

Eugster H. P. and Hardie L. A. 1978. Saline lakes, In Lerman A.(Ed.), Lakes, Chemistry, Geology and Physic. Springer Verlag. 237-293.

Eugster H. P. 1980. Geochemistry of evaporitic lacustrine deposits. Annual Review of Earth and Planetary Sciences, 8: 35-63.

Golobocanin D. ŠKrbic D. and Miljevic R. 2004. Principal component analysis as a tool to indicate the origin of potentially toxic elements in soils. Geoderma, 128: 289-300.

Hao C. Zhang W. and Gui H. 2020. Hydrogeochemistry characteristic contrasts between low- and high-antimony in shallow drinkable groundwater at the largest antimony mine in Hunan Province China. Applied Geochemistry, 117: 104584.

Ibrahim H. Yaseen Z, M. Scholz M. Ali M. Gad M. Elsayed S. Khadr M. Hussein H. Ibrahim H. H. and Eid M. H. 2023. Evaluation and prediction of groundwater quality for irrigation using an integrated water quality indices, machine learning models and GIS approaches: A representative case study. Water, 15: 694.

Kai Z. Jing-xian Q. Yi C. Bai-heng M. Li Y. Hua-ming G. Xin-zhou W. Lin-ying W. and Hai-tao L. 2021. Hydrogeochemical characteristics of groundwater and pore-water and the paleoenvironmental evolution in the past 3.10 Ma in the Xiong'an New Area, North China. China Geology, 4: 476–486.

Kim J. H. Kim K. H. Thao N. T. Batsaikhan B. and Yun S. T. 2017. Hydrochemical assessment of freshening saline groundwater using multiple end-members mixing modeling: A study of Red River Delta aquifer, Vietnam. Journal Hydrology, 549: 703–714.

Krinsely D. B. 1970. A geomorphological and paleoclimatological study of the playas of Iran. Washington, U.S. Gov. Print. Off, 51 OP; H.T.4, 172 III US, 486p.

Li J. Li T. Ma Y. and Chen F. 2022. Distribution and origin of brine-type Li-Rb mineralization in the Qaidam Basin, NW China. China Earth Science, 65 (3): 477–489.

Miller N. and Miller C. 2000. Statistics and chemometrics for analytical chemistry. Pearson Education, Englewood Cliffs, New Jersey. 288.

Mollema P. N. Antonellini M. Dinelli E. Gabbianelli G. Greggio N. and Stuyfzand P. J. 2013. Hydrochemical and physical processes influencing salinization and freshening in Mediterranean low-lying coastal environments. Applied Geochemistry, 34: 207–221.

Montoya S. 2018. What is a Piper diagram for water chemistry analysis and how to create one? Retrieved from https://www.hatarilabs.com/ih-en/what-is-a-piper-diagram-and-how-to-create-one.

Pakzad H. R. and Ajalloeian R. 2004. Geochemistry of the Gavkhoni Playa lake brine: Carbonates and Evaporates, 19: 67–74.

Piper A. M. 1944. A graphic procedure in geochemical interpretation of water analyses. Transactions American Geophysics Union, 25: 914–928.

Qin X. Ma H. Zhang X. Hu X. Li G. and Jiang Z. 2021. Origin and evolution of saline spring water in north and Central Laos based on hydrochemistry and stable isotopes (δD, δ18O, δ11B, and δ37Cl). Water, 13 (24): 3568.

Rosenberg YO. Sade Z. and Ganor J. 2018. The precipitation of gypsum, celestine, and barite and coprecipitation of radium during seawater evaporation. Geochim Cosmochim Acta, 233:50–65.

Salem Z. E. ElNahrawy A. Attiah A. M. and Edokpayi J. N. 2022. Vertical and spatial evaluation of the groundwater chemistry in the Central Nile Delta Quaternary aquifer to assess the effects of human activities and seawater intrusion. Forties Environmental Science. 10:15.

Satheeskumar V. Subramani T. Lakshumanan C. Roy P. D. and Karunanidhi D. 2021. Groundwater chemistry and demarcation of seawater intrusion zones in the Thamirabarani Delta of south India based on geochemical signatures. Environmental Geochemistry Health, 43: 757–770.

Simeonov V. Massart D. L. Andreev G. and Tsakovski S. 2000. Assessment of metal pollution based on multivariate statistical modeling of 'hot spot' sediments from the Black Sea. Chemosphere, 41: 1411-1417.

Stiff H. A. Jr. 1951. The interpretation of chemical water analysis by means of patterns. J. Pet. Technol, 3:15–17.

Torshizian H. Mollai H. Kalani M. and Javanbakht M. 2009.

Hydrogeochemical analysis of the Siyah-kuh district playa brines, Central Iran. Neues Jahrbuch für Geologie und Paläontologie – Abhandlungen. 253: 281-292.

Tranvi L J. Downing JA. Cotner JB. Loiselle SA. Striegl RG. Ballatore TJ. and Dillon P. 2009. Lakes and reservoirs as regulators of carbon cycling and climate. Limnol Oceanogr, 54(6): 2298–2314.

Unglert K. Radić V. and Jellinek A. M. 2016. Principal component analysis vs. self-organizing maps combined with hierarchical clustering for pattern recognition in volcano seismic spectra. Journal Volcanology Geothermal Research, 320: 58–74.

Warren J. 2006. Evaporates: Sediment, Resources and Hydrocarbons. Springer. 1036 p.

White K. and N. Drake 1993. Mapping the distribution and abundance of gypsum in southcentral Tunisia from Landsat Thematic Mapper data. Zeitschrif fur Geomorphologie, 37: 309-325.

Xiao J. Wang L. Chai N. Liu T. Jin Z. and Rinklebe J. 2021. Groundwater hydrochemistry, source identification and pollution assessment in intensive industrial areas, eastern Chinese loess plateau. Environment Pollution, 278: 116930.

Yuan X. Meng F. Zhang X. Sheng J. Galamay A. and Cheng H. 2021. Ore-forming fluid evolution of shallow polyhalite deposits in the Kunteyi Playa in the north Qaidam Basin. Frontiers in Earth Science, 9:125-139.